Supporting information

Corrugated Epsilon-Near-Zero Saturable Absorber for High-performance 1.3 μm Solid-state Bluk Laser

Mengxia Wang,[a,b,c] Hang Jiang,[a,b,c] Hao Ma,[a,b,c] Chuanrui Zhao,[d] Yuanan Zhao,*[a,b,c] Zhengping Wang,*[d] Xinguang Xu[d] and Jianda Shao*[a,b,c,e]

a. Laboratory of Thin Film Optics, Shanghai Institute of Optics and Fine Mechanics, Chinese Academy of Sciences, Shanghai, 201800, China
b. Center of Materials Science and Optoelectronics Engineering, University of Chinese Academy of Sciences, Beijing 100049, China
c. Key Laboratory of Materials for High Power Laser, Chinese Academy of Sciences, Shanghai 201800, China
d. State Key Lab of Crystal Materials, Shandong University, Jinan, 250100, China
e. Hangzhou Institute for Advanced Study, University of Chinese Academy of Sciences, Hangzhou, 310024, China
*Corresponding Author: yazhao@siom.ac.cn; zpwang@sdu.edu.cn; jdshao@siom.ac.cn

S1. Planar ITO film

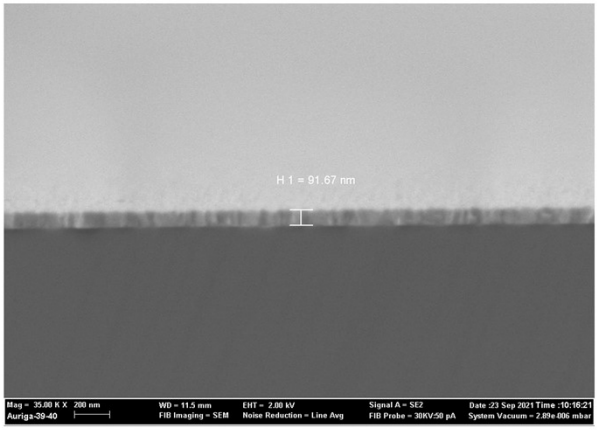

Figure S1. SEM image of planar ITO film deposited under the same process conditions as CITO film.

S2. The extraction of Drude parameters.

The transmittance spectra of ITO and CITO films are measured for extracting the Drude parameters (Figure S2). The characteristic valleys in the transmittance spectra can be used to determine the Drude parameters [1]. In theNIR region, the permittivity of TCOs is described by the Drude model:

$$\varepsilon(\omega) = \varepsilon_{\infty} - \frac{\omega_p^2}{\omega^2 + i\gamma\omega} \quad (1)$$

where ε_∞ is the high-frequency permittivity, ω is the optical angular frequency, ω_p is the plasma frequency, and γ is the damping factor.

The transmittance spectra of ITO and CITO films were obtained at an incident angle of 30° and 0°, respectively. The Drude model and the transfer matrix method are packed as a function to curve-fit the measured transmittance spectra to obtain the Drude parameters.

For planar ITO film, the theoretical transmittance spectrum can be obtained by Drude model and transmission matrix method, the detailed models and methods can be found in reference [1]. The transmittance of ITO film can be obtained [1]:

$$T = \frac{n_2 \cos\theta_2}{n_0 \cos\theta_0}\left|\frac{1}{D_{11}}\right|^2 \tag{2}$$

$$D_m = \begin{bmatrix} \cos\theta_m & -\cos\theta_m \\ n_m & n_m \end{bmatrix} \tag{3}$$

where m = 0, 1 ,2 indicates the layer number; n_m and θ_m are the complex refractive index and the propagation angle of light in the medium, respectively.

Based on this, the Drude parameters (plasma frequency ω_p and damping factor γ) of the planar ITO film were finally obtained by fitting the experimental spectral curve with fmincon function.

For CITO film, the theoretical transmittance spectrum is obtained by Drude model and finite-difference time-domain method because the analytical expression of the transmittance of CITO film cannot be obtained under the condition of subwavelength structure. In order to extract Drude parameters of CITO films, ω_p and γ were sampled by interpolation, and, so as to obtain the best fitting parameters. Fig. S2(a) and S2(b) show the experimental and theoretical transmittance of ITO and CITO films, which are in good agreement with each other. Table S1 shows the fitting Drude parameters of ITO and CITO films.

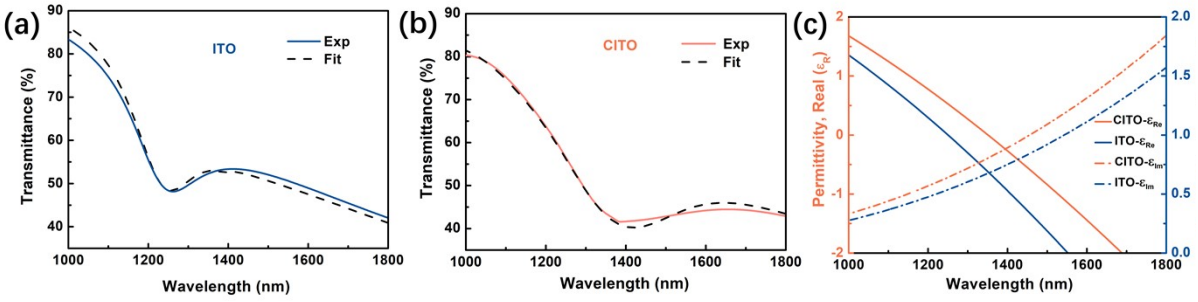

Figure S2. (a) Transmittance spectra of ITO at TM polarization with incident angle of 30°, (b) Transmittance spectra of CITO film at normal incidence, (c) Real part (solid line) and imaginary part (dashed line) of the extracted permittivity for the flat ITO and structural CITO films.

Table S1 Fitting parameters of the Drude model for the ITO and CITO films.

Samples	ε_∞	ω_p (rad/s)	γ (rad/s)
ITO	3.8055	2.96×10^{15}	2.13×10^{14}
CITO	3.8055	2.78×10^{15}	2.95×10^{14}

According to the Drude parameters and Drude model, the permittivity ε of ITO and CITO films can be obtained, as shown in Fig S2(c). It should be pointed out that the high frequency permittivity ε_∞ of ITO and CITO films used in the Drude parameter fitting process are reported in the past. [2] The ENZ wavelength λ_{ENZ} is obtained by solving $\varepsilon_{Re} = 0$ [1]:

$$\lambda_{ENZ} = \frac{2\pi c}{\sqrt{\omega_p^2/\varepsilon_\infty - \gamma^2}} \tag{4}$$

S3. Z-scan experimental

In the Z-scan experiments, the repetition rate was 1 kHz in this work, which is not enough to produce the thermal lens effect according to the related research [3-5]. The incident laser was divided into two beams through a beam splitter. One beam was irradiated on the CITO and ITO samples after passing through a focusing lens, and the other beam was used as a reference light under the same conditions. The sample was placed on a mobile platform that moved along z direction and controlled by a computer. The final experimental data were collected by two power meters (Ophir).

For 1700 nm, the calculated LSPR field enhancement is shown in Figure S3.

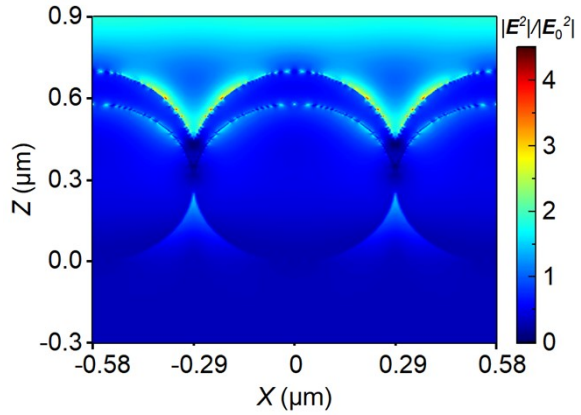

Figure S3. Calculated LSPR field enhancement of CITO at 1700 nm.

The saturable absorption response of the CITO film in the TM and TE polarization states with incident angles in the range of 0–60° are shown in Figure S4.

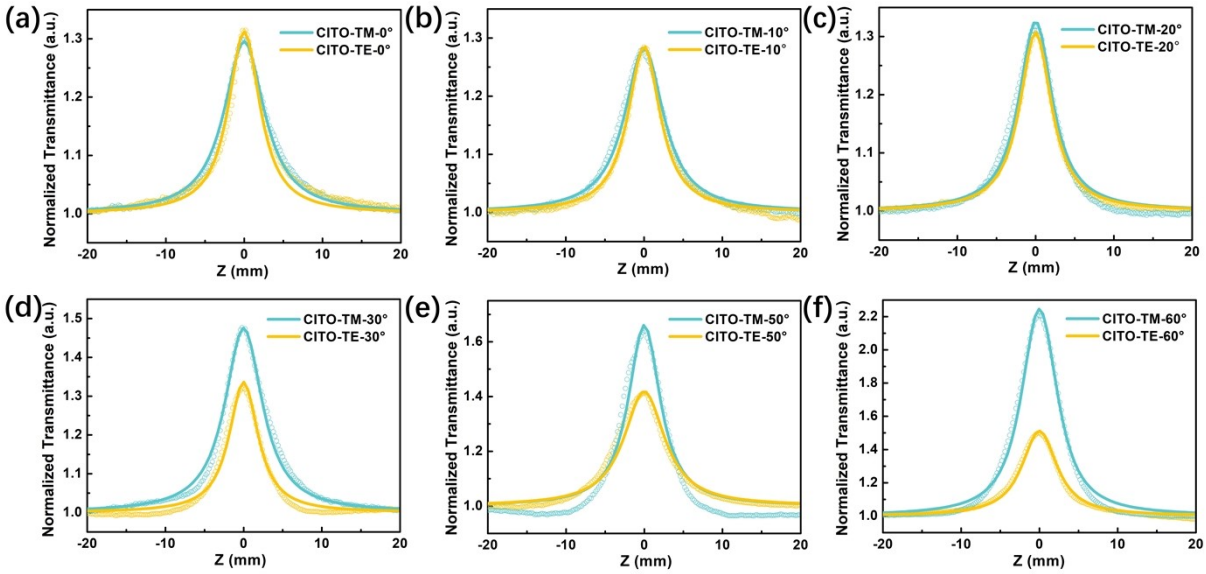

Figure S4. Z-scan curves of CITO film at TM and TE polarization states with incident angles of (a) 0°; (b) 10°; (c) 20°; (d) 30°; (e) 50°; (f) 60°.

S4. Laser damage threshold (LIDT) measurement

The LIDT of CITO were investigated by an 800 nm Ti:sapphire laser system (pulse duration 150 fs, repetition rate 10 Hz) with an energy of up to 6 mJ. Figure S5 shows the schematic of the experimental setup for laser damage and laser conditioning. The energy attenuator was realized by a half-wave plate and polarizer. The beam was focused on the sample through the lens with a focal length of 75 cm. The effective area of the laser spot on the sample was 0.087 mm^2. The Rayleigh length was up to ~5 cm. The surface damage of the CITO sample was diagnosed in real-time with a CCD placed orthogonally in the direction of laser propagation.

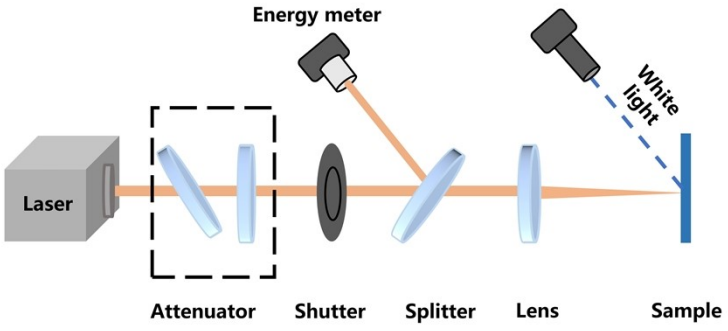

Figure S5. Schematic of laser damage experimental.

References

[1] X. Dai, H. Wang, L. Sun, C. Meng, S. Li and W. Zhang, A*ppl. Optics*, 2021, **60**, 9774–9779.
[2] H. Jiang, Y. Zhao, H. Ma, Y. Wu, M. Chen, M. Wang, W. Zhang, Y. Peng, Y. Leng, Z. Cao and J. Shao, *ACS nano*, 2022, **16**, 12878–12888.
[3] A. Shehata and T. Mohamed, *J. Opt. Soc. Am.* B, 2019, **36**, 1246–1251.
[4] M. Falconieri, *J. Opt. A Pure Appl. Opt.*, 1999, **1**, 662.
[5] A. Gnoli, L. Razzari and M. Righini, *Opt. Express*, 2005, **13**, 7976–7981.